

# Flexural Behaviour of Two-Way Slabs Reinforced using Welded Wire Mesh

Rasha T.S. Mabrouk<sup>\*1</sup>, El-Sayed S. Ewida<sup>2</sup>, Nasser El-Shafey<sup>3</sup>, Akram M. Torkey<sup>4</sup>

<sup>\*1</sup>Ph.D. Associate Professor, Structural Engineering Department, Faculty of Engineering, Cairo University

<sup>2</sup>Ph.D Student, Structural Engineering Department, Faculty of Engineering, Cairo University

<sup>3</sup>Ph.D. Associate Professor, Structural Engineering Department, Faculty of Engineering, Cairo University

<sup>4</sup>Ph.D. Professor, Structural Engineering Department, Faculty of Engineering, Cairo University

Emails: [yrasha@cu.edu.eg](mailto:yrasha@cu.edu.eg)

**Abstract-** This paper is the second part of a research program that studies the behavior of concrete solid slabs reinforced using welded wire mesh and the effectiveness of using welded wire meshes as an economic replacement to ordinary steel bars. This paper focuses on two-way solid slabs where nine two-way simple specimens were tested using concentrated, line, and uniform loading setup. The parameters studied were the effect of using welded mesh and the number of layers utilized. Following that, a finite element analysis using the ABAQUS 6.13 program was conducted. Comparison between the experimental and analytical results showed good correlation. The results showed that the number of layers of welded metal-mesh and load type have a significant effect on the capacity of the slabs. The specimens with welded wire mesh showed higher capacities than that with ordinary reinforcing bars as well as an enhanced cracking behavior and improved ductility. A correction factor is introduced to take the effect of the welding of the wire mesh on the behavior of the concrete slabs. A comprehensive parametric study using 432 slabs was done to investigate the effects of the slab geometry, reinforcement arrangement and the concrete compressive strength. Based on the parametric study, simplified design charts were proposed which can be used as a base for the design of solid slabs reinforced using welded wire mesh.

**Keywords:** Welded wire mesh, Two-way slabs, Ductility, Design charts, Abaqus

## 1. INTRODUCTION

Slabs represent an important element in reinforced concrete structures. Different types of reinforcement can be used with slabs such as reinforcing bars, welded wire steel mesh or fiber reinforcements. The use of welded wire mesh (WWM) has many advantages. It can provide smaller diameter bars with tighter spacing thus leading to an efficient stress transfer to concrete. As a result, the crack width is reduced and the bond between steel and concrete is also increased. The use of WWM largely improves the site efficiency where less manpower is needed since the mesh is produced at the factory thus no bending or shaping is needed on site. The construction cost can be significantly reduced due to the rapid speed of construction and placing of the reinforcement as well as minimizing the waste. In addition, less storage area is needed. Welded wire mesh (WWM) is widely used with ferrocement concrete generally for strengthening or repair of structures. Many types of Welded wire mesh (WWM) are available in the markets with variable sizes and shapes. However, the use of welded wire mesh (WWM) as an alternative reinforcement for solid slabs has been scarcely studied.

Researchers studied the mechanical properties and structural behavior of welded wire mesh. Carrillo et al. [1]

developed a research program to assess the mechanical properties of the welded wire mesh available in their home country. The main parameters studied in the experimental program such as yield stress and strain, ultimate strength strain, elongation, and reduction of cross-sectional area after fracture, shear strength of welding and bending test, were reported, and discussed. Tanawade and Modhera [2] conducted tension stresses on welded and hexagonal wire mesh with the different sizes available in their market. They reported that mesh with 0o orientation gave better results and that the hexagonal mesh showed better ductility.

Welded wire mesh is commonly used with ferrocement concrete used with different structural elements. Leeanansaksiri et al. [3] reported that ferrocement can be used in different applications and being lighter than traditional concrete by 70% makes it suitable for low-cost housing. Ali et al. [4] studied one-way ferrocement slabs under flexure where the slabs were reinforced with a combination of wire mesh and steel fibers. They studied the number of mesh layers as a main parameter, and they concluded that the increase of the wire mesh layer combined with the enhanced distribution along the thickness of the slabs lead to an increase in the capacity and an improvement in the ductility of the slabs. In addition, Banduke and Narule [5] studied one-way ferrocement slabs under bending and punching loading arrangements. They used two types of mesh: square welded mesh and chicken mesh. The parameters under study were the volume fraction and the thickness of the specimens. They concluded that the welded wire mesh showed better flexural behavior compared to the chicken mesh, but the opposite occurred under punching stresses. Phalke and Gaidhankar [6] studied flat ferrocement panels using different types of wire mesh and different number of layers varying from two to four layers. The addition of steel fiber to the mix was also a parameter under study. The panels were tested under two-point loading and the test result shows that panels with a greater number of layers exhibit greater flexural strength, less deflection, better ductility, and energy absorption compared to panels having less no of layers of mesh. In addition, the use of steel fiber enhanced the capacity and behavior of the concrete panels. Rahman and Awal [7] also studied the effect of the wire mesh on the ferrocement slabs using different types of wire mesh with one, two and four layers. They concluded that slabs made with two layers of expanded wire mesh showed the best combination both in terms of strength and cost of material.

The use of welded wire mesh can be expanded where Shaheen and Eltehawy [8] introduced a new pre-cast U shaped ferrocement form as an alternative to the conventional

reinforced concrete slabs. They studied 10 slabs with dimensions of 500x100x2500 mm incorporating 40 mm thick U-shape permanent ferrocement forms. Different types of reinforcing mesh were used. They concluded that using welded galvanized steel mesh gave the highest capacity and improved the energy absorption.

Although considerable research dealt with welded wire mesh used with ferrocement concrete, there isn't much study on the application of welded wire mesh in ordinary concrete. Vigneshwar P. V. and Lenin [9] studied high strength concrete specimens which included conventional reinforced concrete one-way slabs and slabs reinforced using welded wire mesh. They concluded that the strength of welded mesh slab is much greater than the conventional slab and the two types of reinforcement gave different cracking patterns. Li et al. [10] examined ultra-high-performance concrete (UHPC) slabs under blast loads. The slabs were reinforced using four combinations of reinforcement including fiber material and steel wire mesh where only fiber reinforcement, hybrid fiber and steel wire mesh, only steel wire mesh with two volume ratios were incorporated. They showed that two-dimensional steel wire mesh can be effective in improving the flexural capacity of the slabs and that the hybrid system of wire mesh and fiber can effectively improve the shear strength resulting in a more ductile behavior. Altouba et. al. [11] discussed the effect of fibers and welded-wire reinforcements on the diaphragm behavior of composite deck slabs. Twelve large-scale composite deck slabs were instrumented and tested in a cantilever diaphragm configuration to assess the effect of fibers and welded wire mesh on the in-plane shear capacity of composite deck slabs. The load deflection results show that the addition of fibers and WWM increased the ultimate in-plane shear capacity and ductility of the slabs relative to the control specimen. For the slabs tested in the strong direction, the use of A 142 mesh resulted in 19% increase in the ultimate in-plane shear capacity and the additions of 5.3 kg/m<sup>3</sup> of synthetic macro-fibers and 15 kg/m<sup>3</sup> of steel fibers increased the ultimate in-plane shear capacity by 20% and 29%, respectively.

Hong and Jung [12] conducted an experimental study on the use of welded bar mats (WBM) (which improve the rib shape, strength, and diameter limits of the existing structural welded wire fabric) in slabs. Ten simple supported and continuous slabs were tested. The type and strength of the reinforcement, and the compressive strength of concrete were varied. The experimental results were compared to the design standards. They concluded that in case where WBM with yield strength of 400 MPa are used in 21 MPa concrete, a performance like that of normal rebar can be expected, but to use higher strength or steel wires of 500 MPa or higher, an improvement in the rib shape is required for the improvement of the bond strength between the orthogonal steel wires. Aljazeera et al. [13] conducted an experimental work studying the flexural behavior of two-way concrete slabs reinforced using carbon fiber-reinforced polymers' (CFRP) grid in comparison with the conventional welded steel wire mesh using self-consolidating concrete. Three aspect ratios were used for the slabs. They concluded that both CFRP and welded steel mesh behaved better in terms of cracking patterns as the aspect ratio of the slab increased and all the tested slabs showed good serviceability performance.

This paper is the second part of a research program that focuses on the study of the behavior of solid slabs reinforced using welded wire mesh under bending. The first part was introduced in a previous paper by the authors [14] where the behavior of one-way slabs was studied. This paper focuses on the flexural behavior of two-way slabs. As seen from the above literature review, there is not much research conducted on the use of WWM with ordinary concrete slabs and even less work is found related to two-way slabs. Welded wire mesh proved effective, yet its usage is still limited to ferrocement concrete where it can be used as a strengthening material or in the construction of some simple structures. The authors would like to expand on the usage of welded wire mesh to ordinary concrete structures. This research is mainly concerned with slabs used in low-cost housing which is currently much needed in Egypt and used welded wire mesh commonly available in the Egyptian market. WWM presents an effective means for the cost reduction of construction and thus can be a viable replacement for ordinary reinforcing bars especially in small span structural elements.

### Research significance

This article focuses on two-way solid slabs reinforced with welded wire metal mesh. Different types of loading are investigated namely, point load, line load, and uniform loads. The slabs were chosen with small spans usually used in low-cost buildings. The study is divided into an experimental program conducted on nine simple two-way slabs reinforced using single and double layers of welded mesh in addition to control specimens using traditional steel bars. And another part is composed of a finite element analysis using the software package ABAQUS where the tested specimens were modeled, and the analytical results compared with the experimental data to assess the suitability of using ABAQUS in the analysis of the two-way solid slabs. Following that a parametric study is conducted to incorporate wider range of values for the parameters studied taking into account the difference in the behavior of welded wire mesh compared to ordinary steel bars. Currently, there are no provisions in the Egyptian design code of practice ECP 203-2018 [15] for the design of concrete structures using welded wire mesh and thus this hinders the process of design using WWM. The goal of the research program is to introduce a design methodology for slabs using WWM as an alternative reinforcement. Figure 1 summarizes the layout of the research program.

## 2. EXPERIMENTAL PROGRAM

### 2.1 Details of Specimens

All the slabs had the same dimensions of 1050x1050xmm and a total thickness of 50 mm. These in plane dimensions give an aspect ratio of 1 for all the slabs.

The slabs were divided into three groups each having three specimens. Within each group, one specimen was reinforced using ordinary reinforcing bar and will be used as a reference specimen. The other two slabs were reinforced using WWM one having one layer and the other having two layers of mesh. The welded wire mesh had bars of diameter 5 mm welded in both directions. The distance between the bars was 50 mm in both directions.

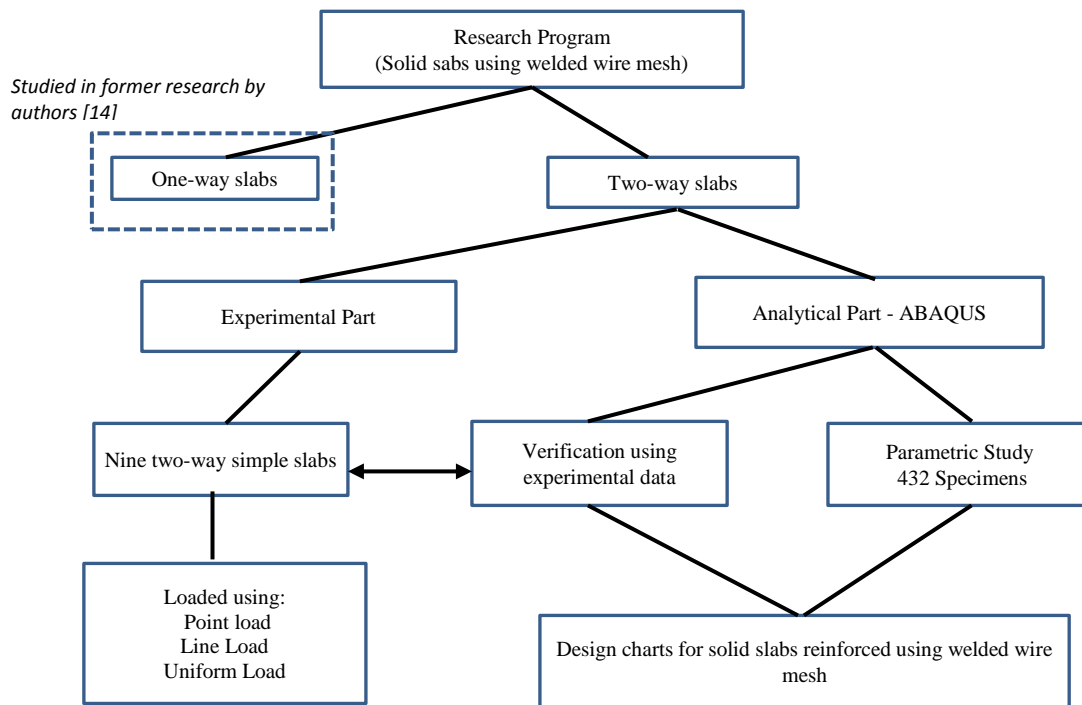



Figure 1. Layout of the research program.

Table 1. Simple two-way slab identification notation and details.

Group No	Specimens	Group No	Specimens	Group No	Specimens	Mesh Type	Reinforcement	F <sub>y</sub> MPa
G1 Point Load	RT-S0-CL	G2 Line Load	RT-S0-LL	G3 Uniform Load	RT-S0-UL	Ordinary steel bars mesh	Φ8@142 mm	368
	FT-S1-CL		FT-S1-LL		FT-S1-UL	WWM One layer	Φ5@50 mm	418
	FT-S2-CL		FT-S2-LL		FT-S2-UL	WWM Two layers	Φ5@50+ Additional Φ5@50 mm	418

Table 2. Mechanical properties of Welded Metal Mesh from manufacture.

Property	Value	(E.S.S) limits, 1109,1971	
Diameter	5 mm	-----	
Yield stress	418 kN/mm <sup>2</sup>	Higher than 240 kN/m <sup>2</sup>	
Ultimate stress	613 kN/mm <sup>2</sup>	Higher than 480 kN/m <sup>2</sup>	
Elongation	20 %	Higher than 20%	

The specimens reinforced with ordinary steel bars and the specimens with one layer of welded wire mesh were designed to have the same reinforcement where the reinforcement ratio for the former was taken as 0.80 % and for the latter as 0.78%. The specimen reinforced with double layer had a ratio of 1.56 % and the additional layer extended over a length of 0.80 L where L is the span of the slab. Figure 2 shows the details of the tested slabs.

The difference between the three groups is in the loading type used for testing where for group one point load is used, for group two, line load is used and for group three uniform load is applied. Table 1 shows the notation used for the specimens. The letters RT refer to the control specimen and the letters FT refer to the specimen having welded wire mesh. The term S0 means ordinary reinforcing bars and S1

means one layer of WWM while S2 means two layers of WWM. CL indicates point load, LL indicates line load, and UL indicates uniform load.

## 2.2 Material properties

The target concrete compressive strength after 28 days was 35.0 MPa. The properties of the mix design are given in the first paper discussing one-way slabs [14]. For the ordinary reinforcing bars mild steel provided from the national companies was used. The diameter used was 8 mm. Laboratory testing was conducted on a sample which gave a yield stress equal to 368 MPa. The welded wire mesh was obtained from a local supplier having a diameter of 5 mm and spacing between bars of 50 mm. Table 2 show the

mechanical properties of the metal mesh. The mesh satisfies the limits set by the E.S.S, 1109-1971 [17].

The specimens were cast in two batches: one for groups 1 and 2 and the other for group 3. Six standard cubes were taken at the time of casting and tested on the same day as the slabs. The average compressive strength of the standard concrete cubes obtained through compressive testing after 28 days was 42 N/mm<sup>2</sup>. Thus, the concrete mix satisfies the target compressive strength of 35 N/mm<sup>2</sup>.

### 2.3 Test setup and instrumentation

To test the specimens as two-way slabs, each specimen was loaded upside down on a rigid metal frame where the frame provides supports to the slabs on all four sides. The

clear span was 1000 mm in both directions. The load was applied through a load cell and a hydraulic jack. The load distribution for the different types of loading was applied using wooden cubes of dimensions 100×100×50 mm as shown in Figure 3. The wooden cubes for line loading were separated every 100 mm along the loading line. Steel channel beams were used to arrange the wooden cubes in a pyramid configuration. For uniform loading, the same arrangement was spaced every 100 mm in both directions, to distribute the jack load evenly to the top slab surface. The deflection was measured using a linear variable displacement transducer (LVDT) at mid span. To gauge the maximum strain in the reinforcement, strain gauges were fixed to the bar at midspan in each specimen.

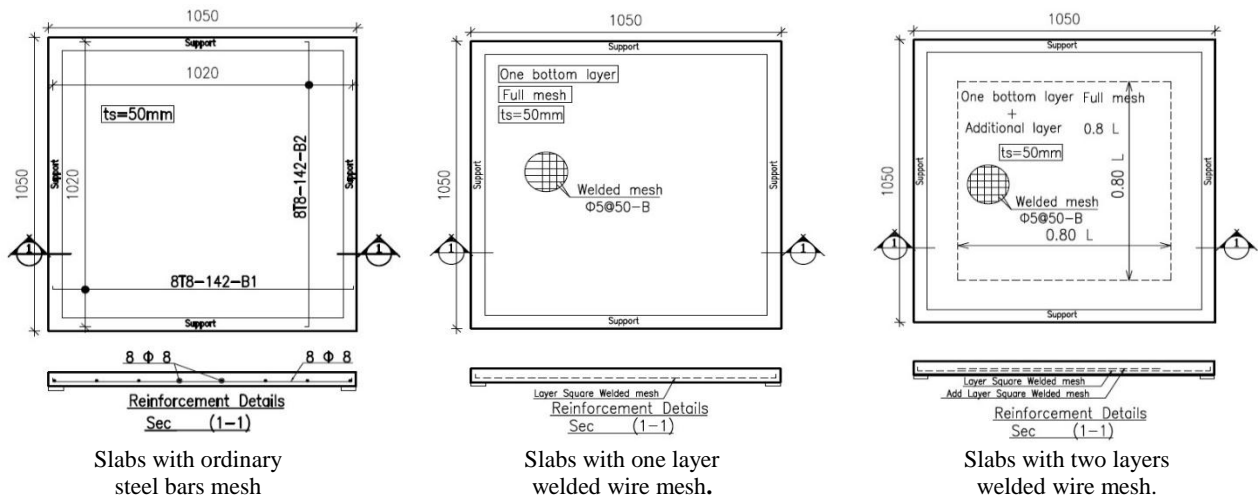
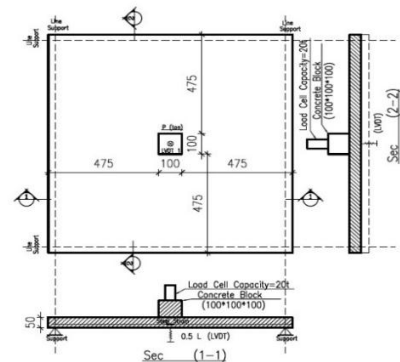


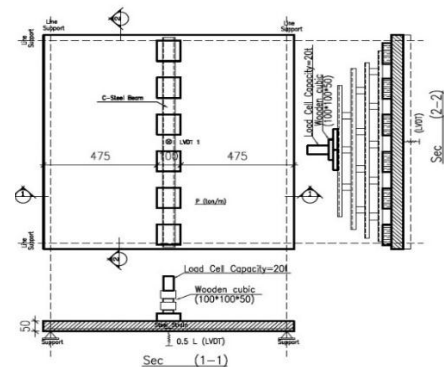
Fig. 2. Details of the different specimens.



a) Concentrated Load



b) Line Load

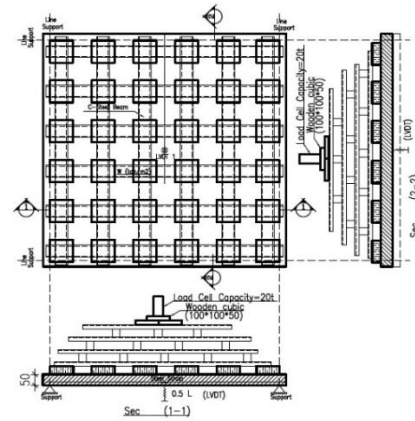






c) Uniform Load

Fig. 3. Test setup under different types of loading.



### 3. TEST RESULTS AND DISCUSSIONS

#### 3.1 Modes of failure and crack patterns

Figure 4 shows the cracking patterns observed at failure for the nine specimens. The general mode of failure observed was flexural failure except for slab FT-S2-CL where punching failure was recorded, and a punching cone was clearly seen. As shown in Figure 4, the cracking patterns for slabs reinforced with welded mesh revealed more cracks distributed around the bottom surface of the specimens with smaller crack widths than in the case of regular reinforcing bars.

**Group 1:** The three specimens in this group were loaded under concentrated load at the center of the slabs. The first cracks generally occurred just under the load and the cracks then extended towards the edges of the slabs in a radial pattern as shown in Figure 4a. This shape of cracks is indicative of bending stresses occurring in both directions of the two-way slabs as intended. For specimen RT-S0-CL, which was reinforced using ordinary steel bars mesh, two major cracks appeared at mid span one in each direction. As the loading increased, the width of cracks increased until the flexural failure occurs. For specimen RT-S0-CL because of the larger spacing between the ordinary bars, larger spacing between cracks were observed. For specimen FT-S1-CL where one layer of WWM was used, the spacing between cracks decreased with smaller width, their number increased compared to RT-S0-CL and flexure failure was also observed. By adding an additional WWM layer in specimen FT-S2-CL, an even larger number of cracks was observed, and the crack width was noticeably decreased. This enhanced crack distribution can be explained due to the better distribution of reinforcement due to the closely spaced bars of the mesh in both directions in case of FT-S1-CL and FT-S2-CL. For Specimen FT-S2-CL, a rather premature failure occurred due to punching.

**Group 2:** The cracking pattern are shown in Figure 4b where they are characterized by a linear pattern in the direction of the applied line load. For specimen RT-S0-LL, two distinct parallel cracks were formed while for specimen FT-S1-LL, there was only one crack, parallel to the line load. In the case

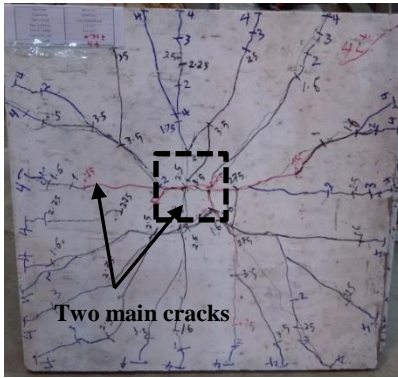
of the double mesh, FT-S2-LL, the quantity of cracks increased and covered the entire surface of the specimen. Flexural failure occurred for all specimens in this group.

**Group 3:** This group consisted of specimens subjected to uniform load. The bottom surface's crack distribution revealed parallel cracks on the slab's two sides. Specimens RT-S0-UL developed a few small cracks and collapsed due to flexure. Specimens FT-S1-UL and FT-S2-UL showed a more evenly spaced crack pattern with FT-S2-UL showing more cracks with smaller width than FT-S1-UL as shown in Figure 4b and 4c. Both specimens failed due to flexural failure.

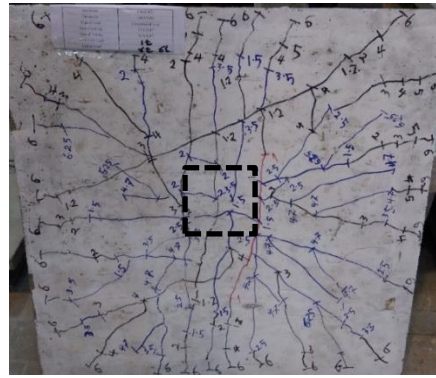
#### 3.2 Load deflection behavior

The test results for the various groups are shown in Table 3 and the load-deflection curves for all specimens are shown in Figure 5. For specimens reinforced with ordinary steel mesh, up until the first crack load, the load deflection curves were found to be linear; after that, non-linearity was seen until failure. For the specimens reinforced with welded wire mesh, the load deflection curves were mostly linear up to the ultimate load and in some specimens, post peak deflection was observed. The loading type did not cause any noticeable difference on the load deflection behavior among the three groups. The first crack load for specimens FT-S1-CL and FT-S2-CL indicate an increase of 33% and 44% for one layer and two layers of mesh compared to the control specimen RT-S0-CL, respectively. While an increase of 33% and 33% was seen for specimens FT-S1-LL and FT-S2-LL, respectively.

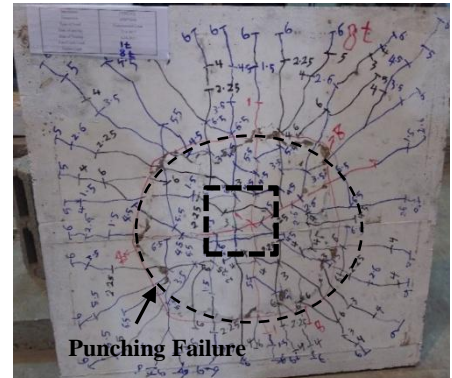
However, for the ultimate load, specimen FT-S1-CL showed an increase about 22% and for specimen FT-S2-CL showed decrease about 4% due to punching failure compared to the control specimen RT-S0-CL while an increase of 52% and 69% was seen for specimens FT-S1-LL and FT-S2-LL. For group 3 under uniform load, specimens FT-S1-UL and FT-S2-UL showed an increase of 25% and 56% for the first crack load compared to the control specimen RT-S0-CL while an increase of 36% and 77% for the ultimate load, respectively. Figure 6 shows the increase in the values of the cracking load and deflection at cracking for all specimens relative to the control specimen in each group.



Specimen RT-S0-CL

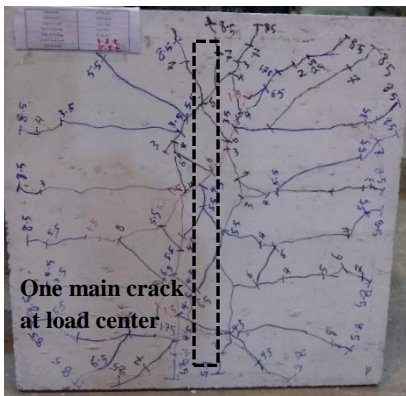


Specimen FT-S1-CL

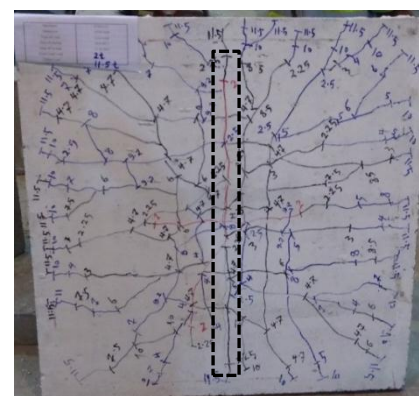


Specimen FT-S2-CL

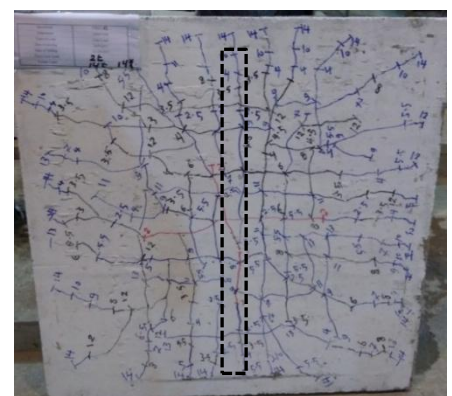
## a) Group 1



Specimen RT-S0-LL

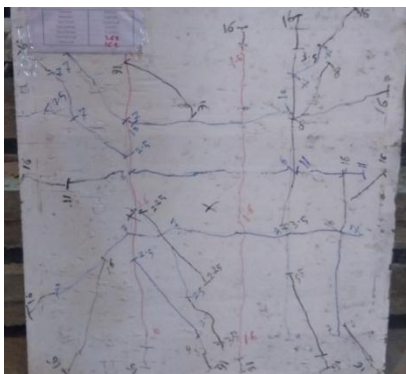


Specimen FT-S1-LL

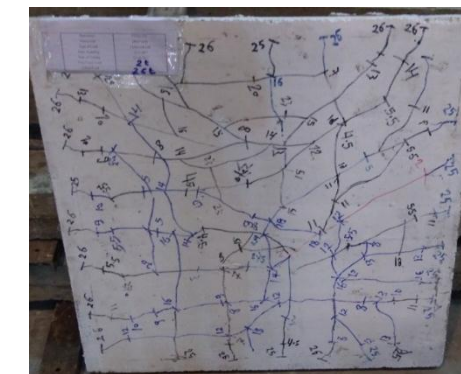


Specimen FT-S2-LL

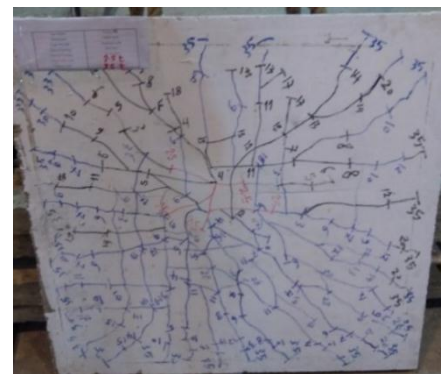
## b) Group 2



Specimen RT-S0-UL



Specimen FT-S1-UL



Specimen FT-S2-UL

## c) Group 3

Fig. 4. Cracking patterns for all specimens at failure.

While Figure 7 shows the ultimate loads and deflections compared to the control specimen. Using one layer of welded wire mesh instead of the ordinary reinforcement showed an increase in the slabs' ultimate capacity and using two layers lead to a significant increase. This is because the presence of the welded wire mesh in both directions has created a grid action which effectively enhanced the slab capacity in addition to the more uniform and close distribution of reinforcement in case of the mesh where the spacing between the bars was 50 mm and their diameter is

only 5 mm. In addition, the values of the deflection increased as the number of welded wire mesh layers increased which shows a significant improvement in the ductility of the slabs when using WWM.

It should be noted that the slabs loaded using uniform loading showed rather large values for ultimate load capacity. This can be explained due to the formation of an arch action during loading that transferred loads directly to the supports. Thus, this loading arrangement needs to be improved if further research is conducted.

### 3.3 Reinforcement load strain behavior

The reinforcement reached the yield strain according to the strain gauge readings for all the specimens except for specimen FT-S2-CL where punching failure was observed. Figure 8 shows specimens load strain curves and the values of strain at ultimate load are given in Table 3. The specimens with ordinary steel mesh generally showed the lowest value of strain which is due to the larger diameter of bars in these specimens with the larger spacing compared to the welded

wire mesh. For all groups under different types of loading, the slabs with ordinary reinforcing bars and the slabs with one layer of mesh showed similar behavior with values of initial stiffness very close to each other. After yielding of reinforcement, the curves started to separate and the specimens with one layer of mesh showed higher load capacity and higher values of strain at the ultimate load. For specimens with double layer, the load strain curve showed nonlinear behavior with an increase in the ultimate strain values.

Table 3. Test results of different groups.

	Test Slabs	$P_{cr}$ (kN)	$\Delta_{cr}$ (mm)	$P_y$ (kN)	$\Delta_y$ (mm)	$P_u$ (kN)	$\Delta_u$ (mm)	(Ultimate Steel Strain) $\times 10^{-6}$
Group 1	RT-S0-CL	7.5	1.77	47.28	7.19	57.22	9.71	2200
	FT-S1-CL	10	2.50	53.97	8.52	69.96	10.12	3700
	FT-S2-CL	10.82	2.47	54.95	8.05	54.95	8.05	1557
Group 2	RT-S0-LL	15	2.00	44.96	4.96	58.95	7.88	2856
	FT-S1-LL	20	3.02	53.05	7.75	89.92	13.07	3080
	FT-S2-LL	20	2.57	92.95	7.07	99.92	11.42	2986
Group 3	RT-S0-UL	16	1.32	122.9	8.71	197.40	12.72	3010
	FT-S1-UL	20	1.36	135.9	8.78	269.86	14.66	4077
	FT-S2-UL	25	1.78	218.6	11.78	349.82	16.58	3863

$P_{cr}$  = First crack load

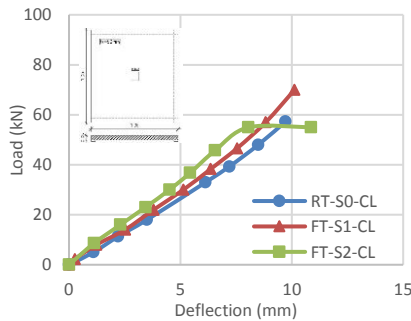
$P_y$  = Load at the yield of steel

$P_u$  = Ultimate load

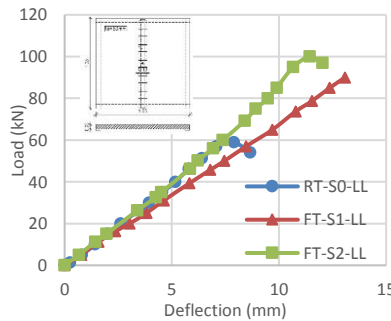
$\Delta_{cr}$  = Cracking deflection.

$\Delta_y$  = Deflection at the yield of steel

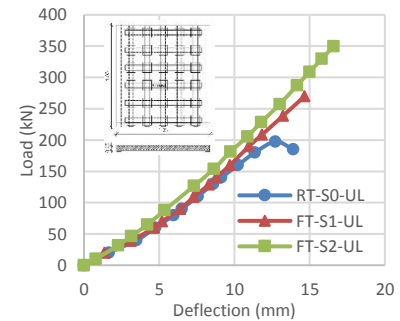
$\Delta_u$  = Ultimate deflection.



a) Group 1

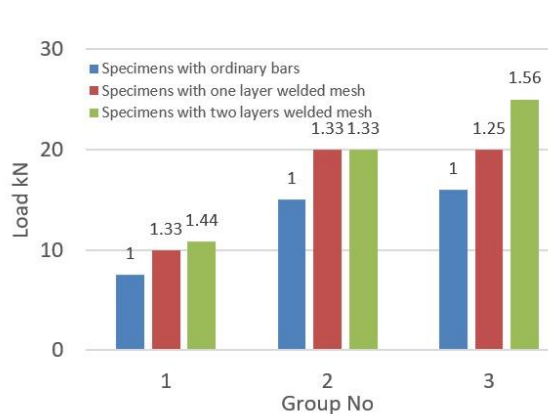


b) Group 2

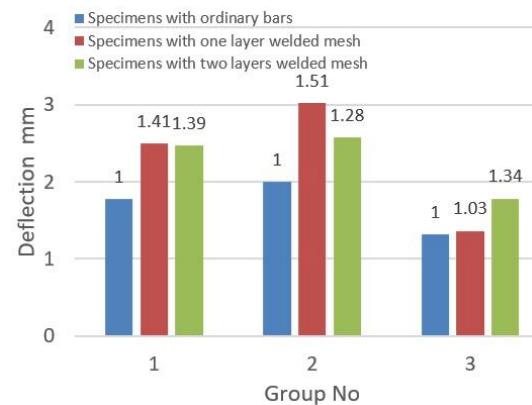


c) Group 3

Fig. 5. Load–deflection curves for the three groups.



a) Cracking load



b) Deflection at cracking load

Fig. 6. Cracking load and deflection results comparison for tested specimens.



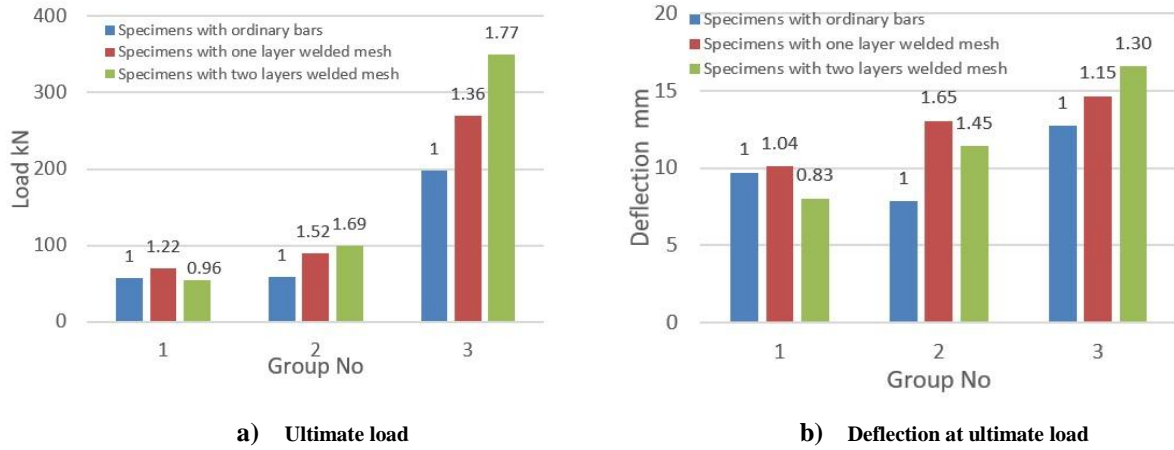


**Fig. 7. Ultimate load and deflection results for tested specimens.**

*Note: Ratios shown in Figures 6 and 7 are relative to the control specimens in each group.*

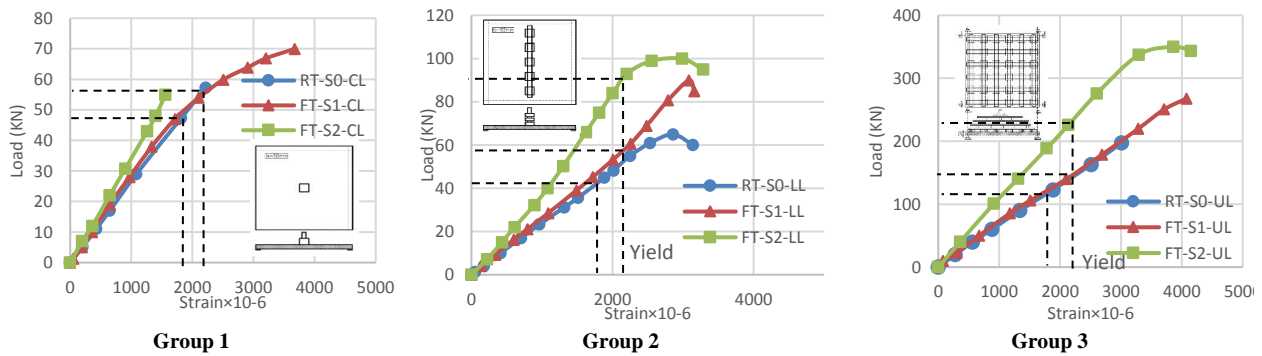


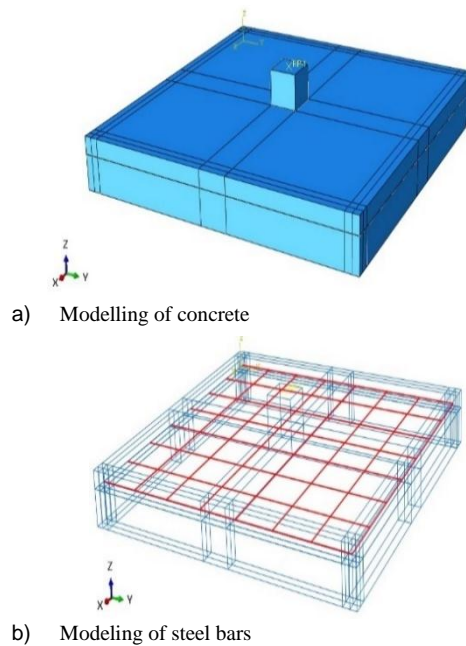
**Fig. 8. Load-strain curves for all specimens.**

#### 4. FINITE ELEMENT ANALYSIS

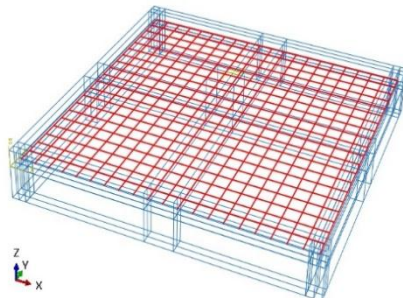
In this part, the nine two-way slabs that were tested experimentally are modeled using the finite element program ABAQUS version 6.13 [18] to assess the validity of using such program in the analysis of concrete slabs reinforced using welded wire meshes. The ABAQUS was used in analyzing one-way slabs in the previous research on one-way slabs [14] and it proved to be a good tool to be used in solving slabs with welded wire mesh. Suitable elements were chosen from the extended ABAQUS library to give the best representation of each of the three elements under study here which are concrete, ordinary reinforcing bars and welded wire mesh.

Concrete was modeled using the element C3D8R where small, uniformly sized mesh elements measuring 50 mm by 50 mm by 5mm were used. T3D2 elements that were included into the surrounding solid elements were used to create steel bars and metal mesh. Figure 9 shows the modeling meshes for the three slab elements. The concrete elements were modelled using the concrete-damaged plasticity model. Elastic plastic modeling was used for the steel bars and the welded wire meshes.

Figure 10 shows the stress strain relationship that was used for concrete while Figure 11 shows the stress strain relationship for steel and welded wire mesh.







c) Modeling of welded metal mesh

Fig. 9. Modeling of different slabs elements

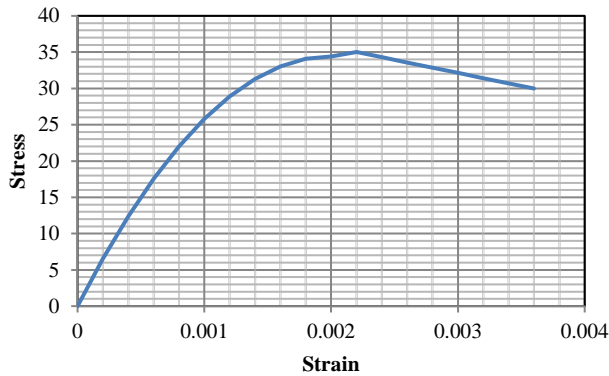


Fig. 10. Stress strain relationship for concrete

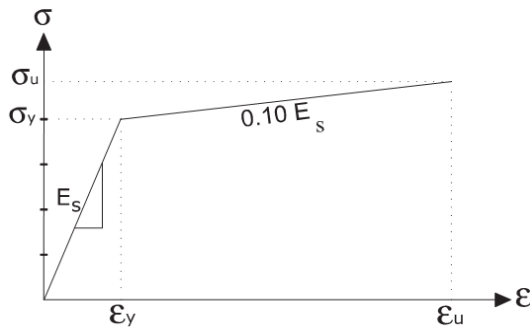


Fig. 11. Stress strain relationship for ordinary steel and welded wire mesh

Table 4. Comparison between experiment (EXP) and finite element model (FEM) at yield.

Group No	Type of Slab	Experimental (EXP)		Finite Element (FEM)		% Diff = $\frac{EXP-FEM}{EXP}$	
		$P_y$	$\Delta_y$	$P_y$	$\Delta_y$	$P_y$	$\Delta_y$
Group 1	RT-S0-CL	47.28	7.19	45.85	6.88	3.02	4.31
	FT-S1-CL	53.97	8.52	50.12	8.12	7.13	4.69
	FT-S2-CL	54.95	8.05	60.11	8.85	-9.39*	18.51
Group 2	RT-S0-LL	44.96	4.96	44.46	4.79	1.11	3.43
	FT-S1-LL	53.05	7.75	48.61	7.43	8.37	4.13
	FT-S2-LL	92.95	7.07	90.2	6.8	2.96	3.82
Group 3	RT-S0-UL	122.93	8.71	89.73	8.32	27.01	4.48
	FT-S1-UL	135.9	8.78	97.9	8.192	27.96	6.70
	FT-S2-UL	218.64	11.78	182.34	11.26	16.60	4.41

\* Punching failure occurred.

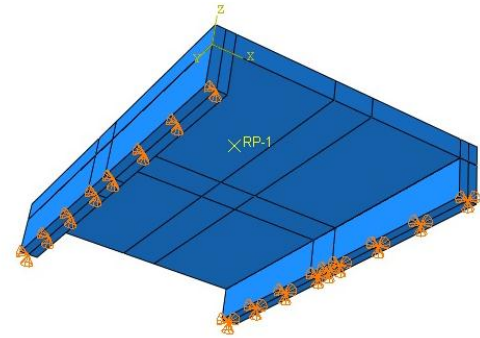


Fig. 12. Boundary condition of FE models

For modeling the welded wire mesh, the modified Ramberg-Osgood curve represented by Equation (1) is used for assessing the tensile stress-strain curve of welded wires as proposed by Ali-Mirza and MacGregor [19]. More details on the finite element modeling and the material parameters used can be referred to in Ewida et al. [14].

$$\varepsilon = \frac{f}{E_s} + \left( \varepsilon_u - \frac{f}{E_s} \right) \left( \frac{f}{f_u} \right)^{20} \quad \text{Equation (1)}$$

Where  $\varepsilon$  is the tensile strain (mm/mm),  $f$  is the tensile stress (MPa),  $f_u$  is the maximum tensile strength,  $\varepsilon_u$  is the strain associated to  $f_u$ , and  $E_s$  is the modulus of elasticity of the material. In this study,  $E_s$  was taken as the value reported by Gere and Goodno [20] where  $E_s = 206000$  MPa.

Figure 12 shows boundary conditions for the finite element models. The exact same conditions applied during the testing of the specimens were represented in the finite element modeling.

#### 4.1 Load deflection behavior

The values of the ultimate load capacity obtained from the numerical analysis using ABAQUS and those measured during the testing of the nine specimens are shown in Table 4 while Figure 13 shows the comparison between the load deflection curves obtained.

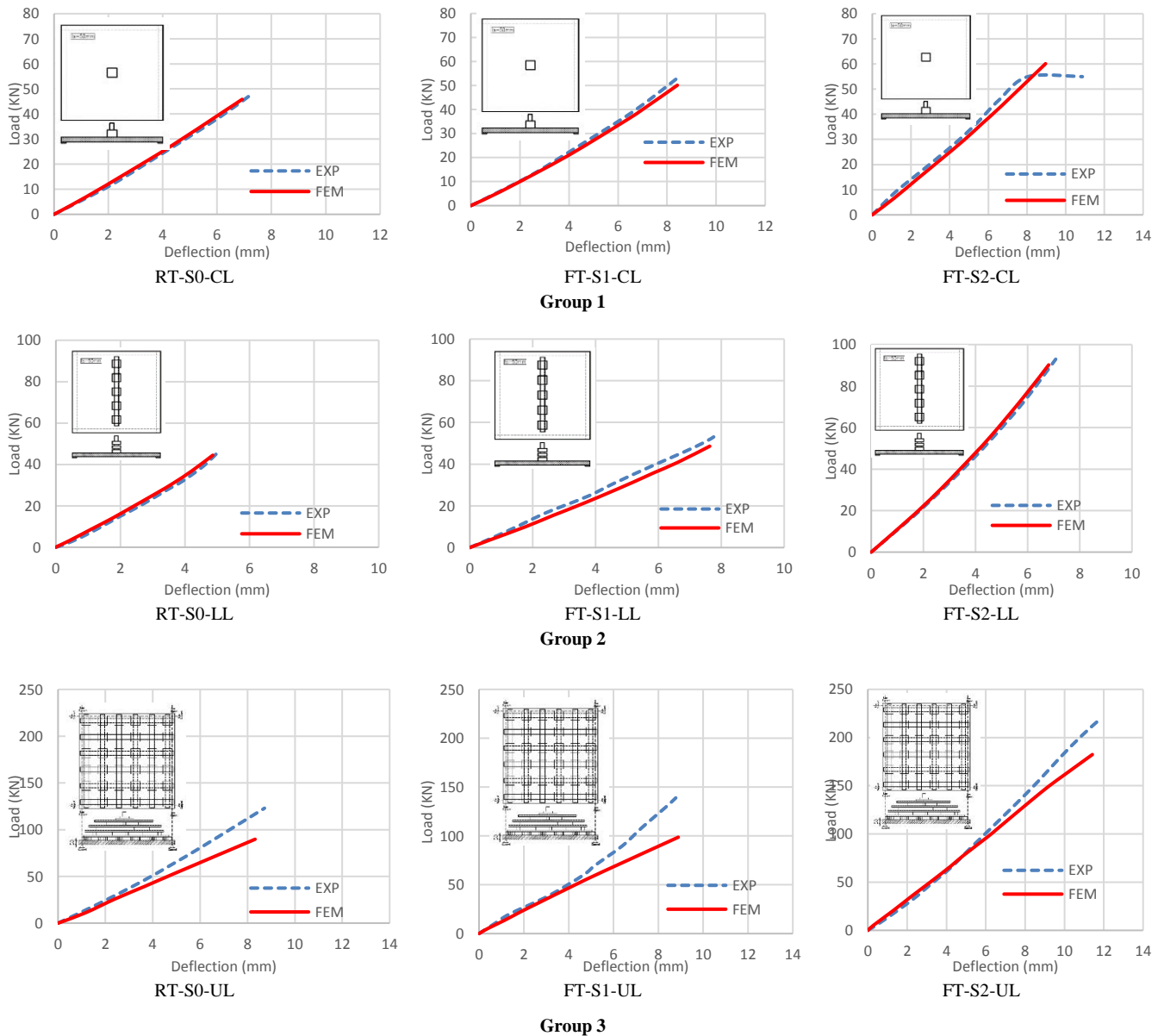


Fig. 13. Load-deflection curves - Comparison between finite element analysis and experiment for tested specimens.

Except for the specimens in Group 3 which are loaded using uniform loading, the maximum difference was about 8% which means that good correlation between the analysis and the experimental results exists and thus showing good performance of the finite element model. For specimen FT-S2-CL, the analytical value of the ultimate capacity was higher than the value obtained from the experiment. This is due to the premature failure that occurred due to punching for this specimen. As for Group 3, the load deflection curves obtained from analysis and experiment are close to each other at the first parts of the curves. As the load increases, a quite large difference of around 28% was obtained. This is due to the rather larger values of ultimate load obtained from experiment for slabs under uniform load. These large values are due to the arch action occurring during loading which led to the overestimated values for ultimate load as explained in section 3.2. The output from the finite element analysis confirms that the values obtained during testing are rather overestimated.

The deviation between the numerical and experimental results can be due to a couple of reasons. First, perfect bond between steel and concrete by simulating steel reinforcement as an embedded component in the concrete at the elastic stage was assumed. Bond degradation was considered at the plastic stage through an empirically derived factor which needs more study as this derived factor may differ from one experimental study to another. Second, the actual stress strain curve for concrete during experiment may slightly differ from the theoretical modeling used depending on the 28 days cube compressive strength. Another main factor that contributes to this difference in values can be because the steel bars in the two directions of the mesh are welded while the modeling using ABAQUS does not take this fact into consideration. The behavior of the welded wire mesh embedded in concrete is quite different from the ordinary steel bars mesh and thus the ultimate load capacity is higher from the experimental data than the finite element analysis

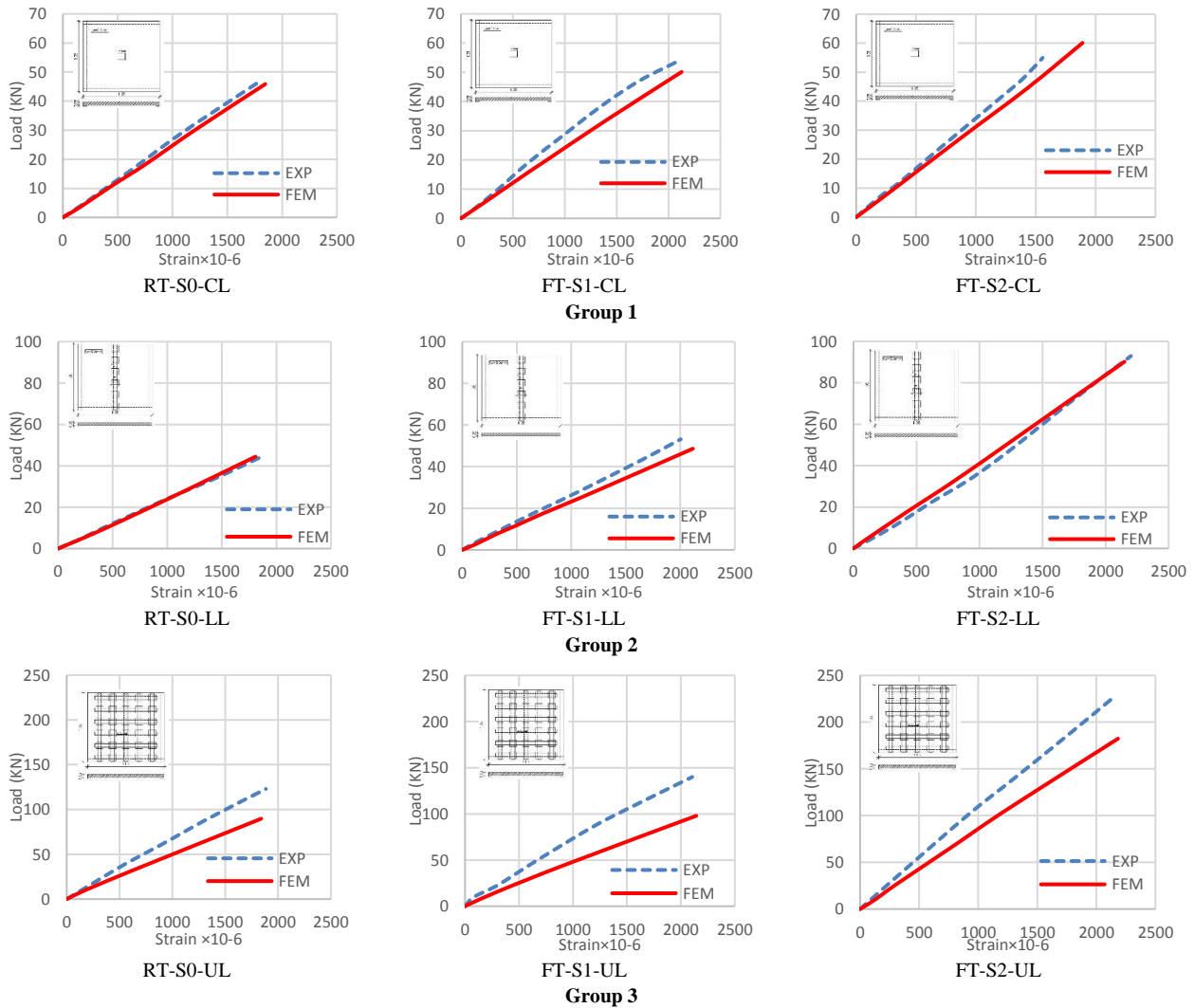


Fig. 14. Load–strain curves comparison between finite element analysis and experiment for tested specimens.

#### 4.2 Load steel strain behavior

Figure 14 shows the comparison between the readings taken during the experimental program and the results of the FEM analysis. In general, the two results are in good correlation. However, numerical analysis readings are generally slightly lower than the readings obtained during the experiment. For Group 1 and Group 2, all specimens reached yield strain with severe cracks observed. For Group 3 (two-way slabs loaded under uniform load), the experimental curves divert more from finite element ones. This again can be explained due to the rather overestimated experimental values.

### 5. PARAMETRIC STUDY AND PROPOSED DESIGN APPROACH

The objective of this section is to formulate a design approach that can be used for solid slabs reinforced using welded wire mesh. Currently there are no provisions in the design codes that details design formulae or procedure for

using welded wire mesh as reinforcement. Only some guidelines on the use of steel mesh with ferrocement [21,22]. Some researchers studied the properties of welded wire mesh under tension, compression, and flexure [23-25] but still no models are available for practical design. The proposed design approach is intended to focus mainly on slabs used in low-cost housing which is currently in large demand in Egypt. In this case slabs of short spans not exceeding 3.5 m are commonly used and the use of less expensive materials is greatly needed which makes slabs reinforced with WWM a very good alternative. The design method will introduce design charts that can be easily used to calculate the load capacity of slabs reinforced with welded wire mesh (WWM).

#### 5.1 Comparison between experimental results and design using equilibrium equations

In this part, a second approach to assess the experimental results of the specimens is introduced. The slabs that were tested experimentally are analyzed using the standard design methods for sections under bending as given by the compatibility and equilibrium equations of the ECP [15] and



then the results are compared with the experimental data previously obtained. The nine two-way slabs introduced in this article as well as nine one-way specimens that were previously studied by the authors [14] were analyzed.

Figure 15 shows the stress and strain distributions for a singly reinforced section under pure bending. By using equilibrium equations, the moment capacity for the section can be calculated using the following equations.

$$M_u = (T \text{ or } C) \times (d - \frac{a}{2})$$

$$= A_s \times \frac{F_y}{\gamma_s} \times (d - \frac{a}{2}) \quad \text{Equation (2)}$$

$$M_u = A_s \times \frac{F_y}{\gamma_s} \times d \times (1 - \frac{a}{2d})$$

$$= A_s \times \frac{F_y}{\gamma_s} \times d \times (1 - \frac{\mu \times F_y \times \gamma_c}{1.34 \times \gamma_s \times F_{cu}}) \quad \text{Equation (3)}$$

$$\mu = \frac{A_s}{b \times d} \quad \text{Equation (4)}$$

Where: -

$M_u$  Ultimate moment capacity.

$a$  Stress block distance.

$F_y$  Yield stress for steel.

$F_{cu}$  Compressive stress for concrete.

$d$  Effective depth of section.

$\mu$  Steel percentage in section.

$\gamma_c$  Material factor of safety for concrete.

$\gamma_s$  Material factor of safety for steel.

Using the moment capacity for the slab cross section, the ultimate load capacity can be obtained by calculating the load for the short direction and for the long direction. The value obtained through the short direction is the most critical of the two as given by Equation (5) and Equation (6). The calculated ultimate load capacity from the previous equations, as well as the experimental load capacity of tested slabs are listed in Table 5.

- Point and line loads for simply supported slabs:

$$M_u = \frac{P \alpha \times A}{4} \quad \text{Then} \quad P_\alpha = \frac{4 \times M_u}{A}$$

$$\text{Then} \quad P_u = \frac{P \alpha}{\alpha} \quad \text{Equation (5).}$$

- Uniform loads for simply supported slabs:

$$M_u = \frac{W \alpha \times A^2}{8} \quad \text{Then} \quad W_\alpha = \frac{8 \times M_u}{A^2}$$

$$\text{Then} \quad W_u = \frac{W \alpha}{\alpha} \quad \text{Equation (6)}$$

Where: -

$M_u$  Ultimate moment capacity.

$A$  Short span.

$\alpha$  Distribution factor in the short direction for two-way slabs obtained using Grashoff's equations [15]

$P_\alpha$  Load for short direction

$W_\alpha$  Uniform load for short direction

The experimental values for specimens reinforced using welded wire mesh exceed that calculated using the equilibrium equations which is in part due to the effect of welding found in the real situation of the experimental tests. However, for specimen FT-S2-CL specimen which failed due to punching, the estimated capacity from equations was greater than experimental one. The average percentage

increase for slabs under concentrated load was about 1.13, while for line load it was 1.10. However, the amount of increase in the case of uniform loading was about 1.28. This high amount of increase may be attributed to the arch action status which was explained earlier leading to overestimated experimental data for slabs under uniform load.

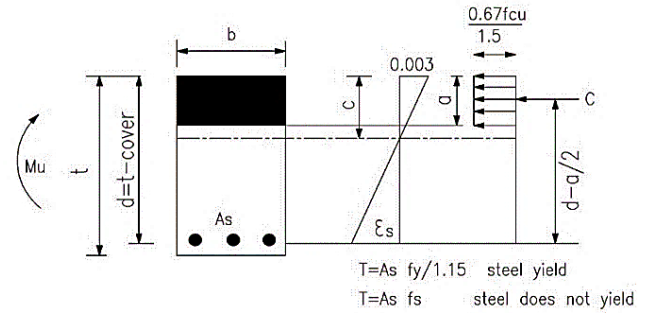


Fig. 15. Stress and strain distributions for a singly reinforced section [15]

Table 5. Load comparison between experimental data (EXP) and equilibrium equations (EE).

Specimen	Load (at yield) (kN)		
	EXP	EE	EXP / EE
<b>One-way slabs ref [14]</b>			
RO-S0-CL	32.83	31.43	1.04
FO-S1-CL	40.72	35.29	1.15
FO-S2-CL	69.96	62.76	1.11
RO-S0-LL	32.98	31.43	1.05
FO-S1-LL	39.27	35.29	1.11
FO-S2-LL	68.96	62.76	1.10
RO-S0-UL	80.80	62.86	1.29
FO-S1-UL	88.94	67.99	1.31
FO-S2-UL	145.13	125.52	1.16
<b>Two-way slabs</b>			
RT-S0-CL	47.28	44.00	1.07
FT-S1-CL	53.97	47.59	1.13
FT-S2-CL	54.95	87.86	0.69*
RT-S0-LL	44.96	44.00	1.02
FT-S1-LL	53.05	47.59	1.11
FT-S2-LL	92.95	87.86	1.06
RT-S0-UL	122.93	88.00	1.40
FT-S1-UL	135.9	95.18	1.43
FT-S2-UL	218.64	175.72	1.24

\* Punching failure occurred.

## 5.2 The welding correction factor ( $\eta$ ).

The behavior of welded wire mesh under flexure is quite different from ordinary reinforcing bar mesh. The authors suggest that the main cause of this difference arises from the welding between the wires in the two directions of the WWM which is done during manufacturing. To calculate the ultimate load for the slabs using WWM, a correction factor is introduced to take the effect of the welding in the two directions of the WWM into consideration. This factor can be defined using the following equation:

$$P_{mod} = \eta \times P_{calc} \quad \text{Equation (7)}$$

Where:

$P_{mod}$ : Calculated load capacity for slabs reinforced with welded mesh.

$P_{calc}$ : Modified load capacity for slabs reinforced with welded mesh.

$\eta$ : Correction factor for considering the welding effect.

To obtain the value for  $\eta$ , comparison between the experimental data and finite element analysis as well as the values obtained using the equilibrium and compatibility equations is performed. A proposed value for the correction value ( $\eta$ ) is introduced. This value can be multiplied by the calculated capacity of slabs reinforced with welded wire mesh under different loading types to give a more accurate estimate of the ultimate capacity. As a tentative assumption the high capacities obtained from the uniform load can be ignored and an average value of 1.1 for  $\eta$  can be assumed for the three cases of loading. It should be indicated that the proposed capacity correction factor ( $\eta$ ) is valid within the studied range and size of specimens, and it needs further investigation which will be introduced in future research by the authors.

### 5.3 Parametric Study

In this section, an extended parametric study is conducted using a wider range of parameters than those used in the experimental program. Different span lengths and rectangularity aspect ratios are used with variable reinforcement ratios as well as variable concrete compressive strengths. 432 slab specimens are studied where the span varied between 2 and 3.5 m and the rectangularity aspect ratio ( $R$ ) was taken as 1, 1.5, 2, and 2.5. Three grades of concrete compressive strength namely 20, 25, 30 N/mm<sup>2</sup> were used with three different types of welded metal mesh: 3@30mm, 5@50mm, and 7@70mm. The yield strength of the mesh was 418 N/mm<sup>2</sup>. These values for the compressive strength are those commonly used for low-cost housing and the three types of WWM are the most commonly available in the Egyptian market. The slab thickness was chosen to comply with Egyptian concrete code for practice requirements [15] and is assumed as 100 mm. Table 6 shows a summary of the details of the 432 specimens used in the parametric study. The 432 slabs were analyzed using the

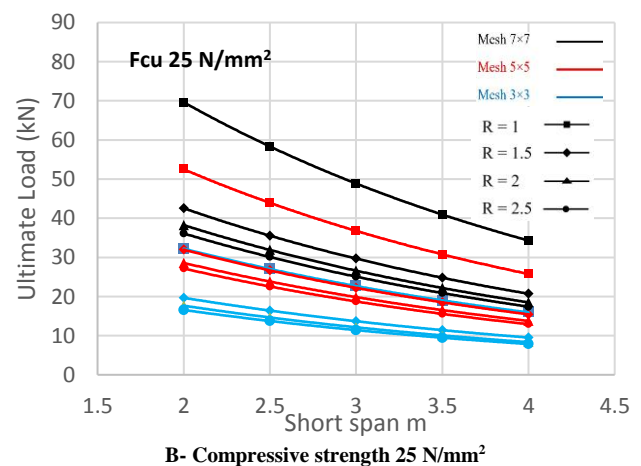
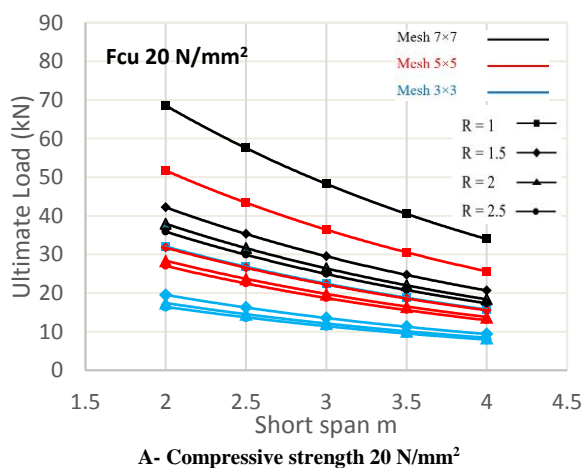
FEM ABAQUS program [18] and the results were analyzed as will be shown in the following section.

**Table 6. Parametric study variables for point, line, and uniform load.**

Variables							
R	Short Span (m)	Fcu 1 MPa	Fcu 2 MPa	Fcu 3 MPa	As 1	As 2	As 3
1	2	20	25	30	Mesh 3@30 mm	Mesh 5@50 mm	Mesh 7@70 mm
	2.5						
	3						
	3.5						
1.5	2						
	2.5						
	3						
	3.5						
2	2						
	2.5						
	3						
	3.5						
2.5	2						
	2.5						
	3						
	3.5						

### 5.4 Proposed design charts for different types of loading.

By solving 432 slab models with different rectangularity ratios using the finite element program ABAQUS, design charts that summarize the relation between ultimate load and short span for slabs loaded by point, line, and uniform load were obtained as shown in Figure 16 to Figure 18. These Figures can be used as a design aid for design slabs reinforced by welded metal mesh. The ultimate load can be obtained from the charts for a certain value of compressive strength based on the short span, rectangularity ratio ( $R$ ) and the type of mesh used. The values of load include material factor of safety which was taken 1.5 for concrete and 1.15 for welded wire mesh. In addition, the welding correction factor ( $\eta$ ) with a value of 1.1 is also incorporated into the results. The design charts are only valid for the range of data studied which is suitable for low cost housing. Further investigation needs to be done for a larger range of parameters if needed.



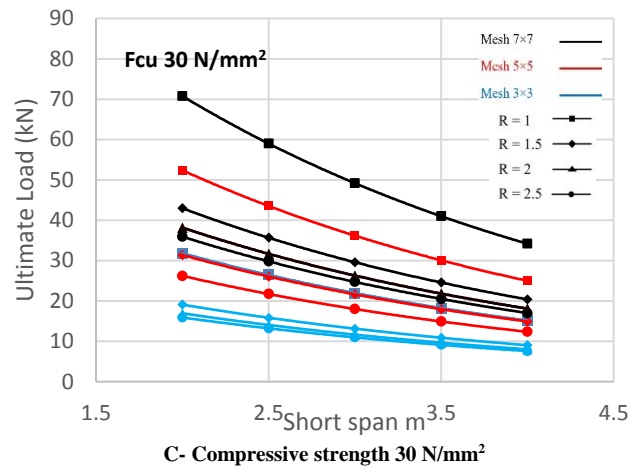
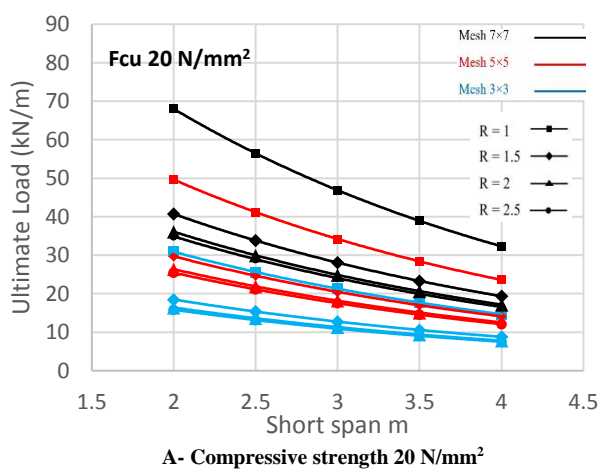
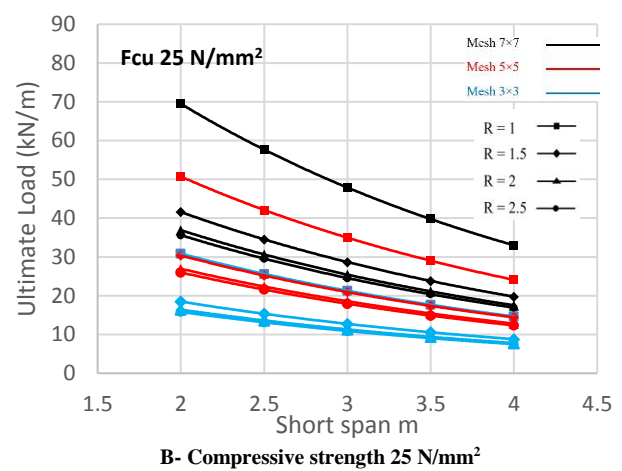


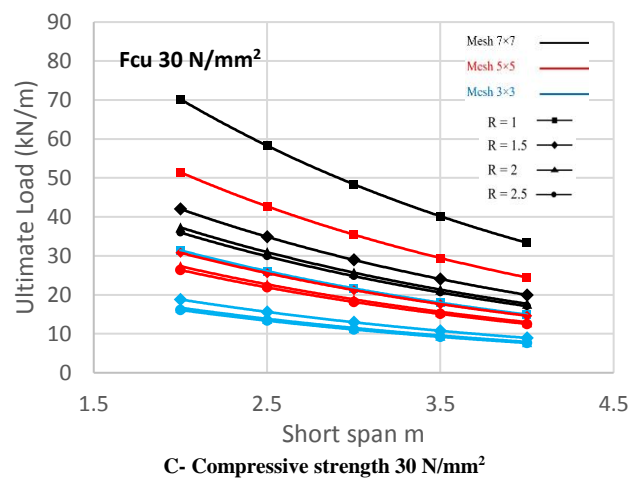
Fig. 16. Relationship between the load and slab span for point load.



A- Compressive strength 20 N/mm²



B- Compressive strength 25 N/mm²



C- Compressive strength 30 N/mm²

Fig. 17. Relationship between the load and slab span for line load.



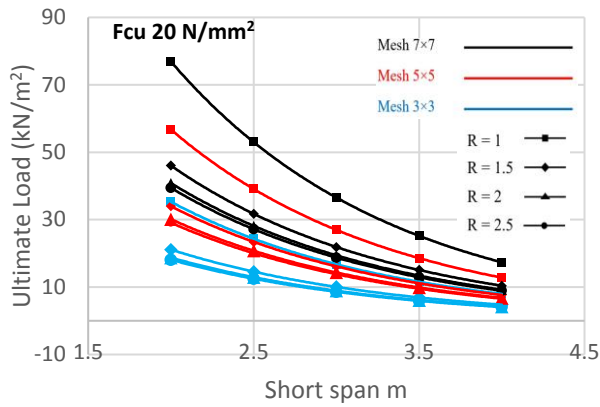
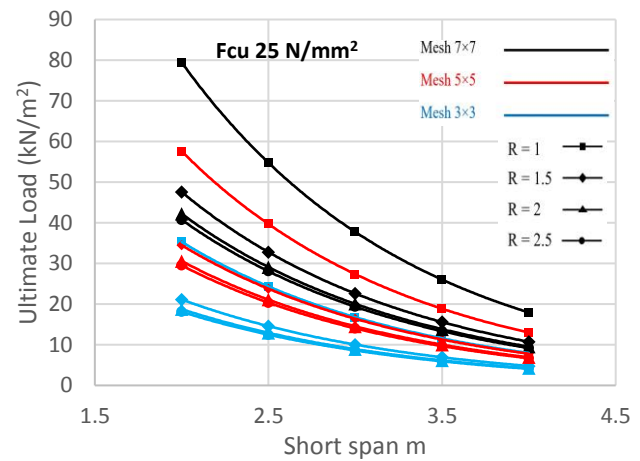
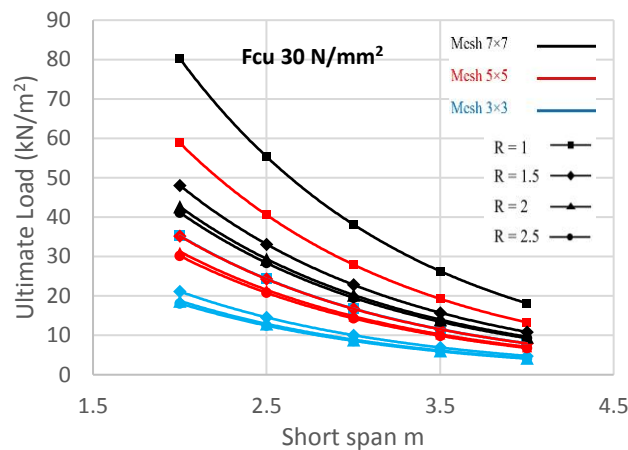
A- Compressive strength 20 N/mm<sup>2</sup>B- Compressive strength 25 N/mm<sup>2</sup>C- Compressive strength 30 N/mm<sup>2</sup>

Fig. 18. Relationship between the load and slab span for uniform load.

## 6. REAL CASE STUDY (LOW-COST HOUSING BUILDING)

In this part an example of one of the common low-cost housing units in Egypt is analyzed using the proposed design charts for slabs with welded wire mesh and the cost estimate is compared with that using ordinary steel bars. The architecture plan for the units chosen is divided into a living area, three rooms, one bathroom and kitchen with a total area of 90 m<sup>2</sup>. The structural system for this model is already available using solid slab reinforced with ordinary steel bars mesh. The slab thickness in this case is 140 mm with reinforcement  $\Phi 10@166$  mm. The same slabs were redesigned using welded wire mesh. The slab thickness was reduced to 100 mm and welded wire mesh of  $\Phi 5@50$  mm was used. The proposed design charts were used in the redesign of the slabs and the quantities of concrete and steel recalculated.

Table 10 shows a comparison between the estimated cost using the two types of reinforcement. The initial cost for the slabs was reduced by about 27.24% (55419.50 EGP) when using welded wire mesh instead of ordinary reinforced bars. This reduction is due to the decrease in the slab thickness and the weight of steel. It should be noted that further reduction

can also be obtained due to other factors such as labor and construction cost reduction as well as the saving in the construction time.

## 7. SUMMARY AND CONCLUSIONS

This study was conducted to investigate the behavior of two-way slabs reinforced using welded wire mesh. The research program was divided into two parts. First an experimental program which included nine two-way solid slabs loaded using point, line, and uniform loads. Second an analytical program using the ABAQUS program where verification of the experimental data was done followed by a parametric study which included 432 slab specimens with different geometry and reinforcement ratios. Based on the data and results obtained the following conclusions can be drawn.

- 1- Welded wire mesh can be used in concrete slabs as a good alternative to ordinary steel bars which lead to a significant increase in the ultimate capacity of the slabs.
- 2- Using welded wire mesh resulted in improved ductility for the tested slabs under flexural loads. It also delayed the appearance of cracks and decreased the crack width, which grew slowly and with better distribution.

Table 10. Cost reduction values for the case study.

Typical Slab	Slab area (m <sup>2</sup> )	Slab Concrete Volume (m <sup>3</sup> )	RFT Details	Weight of steel kg	Cost of reinforcement (EGP)	Cost of concrete (EGP)	Total cost (EGP)
Slab With steel Bars	473	66.22	Bot at (X-X) Φ10@166	3659	53055	99330	203425
			Top at (X-X) Φ10@166	3520	51040		
Slab With Welded mesh	473	47.3	Bot at (Y-Y) FΦ5@50	2327	37232	70950	148006
			Top at (Y-Y) FΦ5@50	2489	39824		
The decrease in cost of concrete				28380 EGP			
The decrease in cost of reinforcement				27039 EGP			
The decrease in Cost For typical slab				55419 EGP			
Typical floor slab cost reduction percentage				27.24%			

**Note:** Materials prices are taken as 14.5 EGP per Kg for steel bars, 16 EGP for welded mesh and 1500 per cubic meter (m<sup>3</sup>) for concrete. All prices are recorded at year 2020-2021 which may vary due to inflation rate.

- 3- Using welded wire mesh in two-way slabs increased the slabs ultimate load capacity by about 14% for concentrated load and 18% for line load and 10% for uniform load compared to slabs reinforced with ordinary bars for the range of specimens used.
- 4- Adding an additional welded wire mesh layer increased the carrying loading capacity for slabs by about 71% for point load, 75% for line load, and 62% for uniform load over the specimen with only one layer.
- 5- Finite element analysis using the ABAQUS program provides an acceptable level of accuracy where the numerical predictions of the ultimate capacities are close to the experimental ones showing the good performance of the finite element model.
- 6- A proposed correction value ( $\eta$ ) can be multiplied by the calculated capacity of slabs reinforced with welded wire mesh under different loading types to take the effect of welding during the manufacturing of the wire mesh. It should be stated that, the proposed factor ( $\eta$ ) is valid within the studied range and size of specimens, and it needs further investigation with large slab sizes.
- 7- Based on the parametric study and the finite element models results, a design approach was developed in the form of charts for estimating the ultimate load capacity for slabs under different types of loading and with different steel areas. These design charts are valid for the chosen range of slab lengths suitable for low cost housing.
- 8- Replacing ordinary steel bars with welded wire mesh in slabs can lead to a considerable cost reduction.

#### Funding:

This research has not received any type of funding.

#### Conflicts of Interest:

The authors declare that there is no conflict of interest.

#### REFERENCES

- [1] Carrillo J., Rico A., & Alcocer S. (2016). Experimental study on the mechanical properties of welded wire meshes for concrete reinforcement in Mexico City. *Construction and Building Materials*, 127, 663-672. <http://dx.doi.org/10.1016/j.conbuildmat.2016.10.011>.
- [2] Tanawade A. G., & Modhera C. D. (2017). Tensile Behaviour of Welded Wire Mesh and Hexagonal Metal Mesh for Ferrocement Application. *Conf. Series: Materials Science and Engineering*, 225, 1-7. doi:10.1088/1757-899X/225/1/012069.
- [3] Leeanansaksiri, A., Panyakap, P., & Ruangrassamee, A. (2018). Seismic capacity of masonry infilled RC frame strengthening with expanded metal ferrocement. *Engineering Structures*, 159, 110-127. doi:10.1016/j.engstruct.2017.12.034.
- [4] Ali Z. H., Hama S. M., & Mohana M. H. (2020). Flexural behavior of one-way ferrocement slabs with fibrous cementitious matrices. *Periodicals of Engineering and Natural Sciences*, 8(3), 1614-1624. <http://dx.doi.org/10.21533/pen.v8i3.1548>.
- [5] Banduke K.V. & Narule G. N. (2019). Study on ferrocement slab with different meshes for flexure and punching shear. *International Journal of Research and Analytical Reviews*, 6(2), 192-195.
- [6] Phalke R. J. & Gaidhankar D. G. (2014). Flexural behaviour of ferrocement slab panels using welded square mesh by incorporating steel fibers. *IJRET: International Journal of Research in Engineering and Technology*, 3(5), 756-763.
- [7] Rahman M. S. & Awal A.S.M.A. (2000). Effect of wire mesh on flexural behaviour of ferrocement slab. *Bangladesh J. Agri. Engg.*, 11 (1&2), 15-21.
- [8] Shaheen, Y. B. I., & Eltehawy, E. A. (2017). Structural behaviour of ferrocement channels slabs for low-cost housing. *Challenge Journal of Concrete Research Letters*, 8(2), 48-64. doi:10.20528/cjcr.2017.02.002.
- [9] Vigneshwar P. V. & Lenin D. (2020). Flexural behaviour of welded mesh reinforced concrete slab. *Technical research organization India*, 7(8), 95-99.
- [10] Li, J., Wu, C., & Liu, Z.-X. (2018). Comparative evaluation of steel wire mesh, steel fibre and high-performance polyethylene fibre reinforced concrete slabs in blast tests. *Thin-Walled Structures*, 126, 117-126. doi:10.1016/j.tws.2017.05.023.
- [11] Altoubat S., Ousmane H. & Barakat S. (2015). Effect of fibers and welded-wire reinforcements on the diaphragm behavior of composite deck slabs. *Steel and Composite Structures*, 19(1), 153-171. DOI: <http://dx.doi.org/10.12989/scs.2015.19.1.153>.
- [12] Hong G. & Jung S. (2022). Flexural Performance Evaluation of Slab Using Welded Bar Mat. *Journal of Asian Architecture and Building Engineering*. DOI: 10.1080/13467581.2022.2066675.
- [13] Aljazaeri Z., Alghazali H. H., & Myers J. J. (2020). Effectiveness of Using Carbon Fiber Grid Systems in Reinforced Two-Way Concrete Slab System. *ACI Structural Journal*, 117(2), 81-89. doi: 10.14359/51720198.
- [14] Ewida E. S., Mabrouk R. S., El-Shafey N. & Torkey A. M. (2022). Flexural behavior of one-way slabs reinforced with welded wire mesh under vertical loads. *Civil Engineering Journal*, 8(4), 654-671. <http://dx.doi.org/10.28991/CEJ-2022-08-04-03>
- [15] ECP 203. (2018). *Egyptian Building Code for Structural Concrete Design and Construction*, Ministry of Housing Utilities and urban Communities, Cairo, Egypt.
- [16] ESS, 4756-11. (2007). *Physical and mechanical properties examination of cement, part 1*. Egyptian Standards Specification, Cairo, Egypt.
- [17] ESS, 1109. (1971). *Egyptian Standards Specification*, Cairo, Egypt.
- [18] ABAQUS v6.13 user manual (2013).

- [19] Carrillo J., Rico A., & Alcocer S. (2016). Experimental study on the mechanical properties of welded wire meshes for concrete reinforcement in Mexico City. *Construction and Building Materials*, 127, 663–672.
- [20] Gere J., & Goodno B. (2013). *Mechanics of Materials*, eighth ed., Cengage Learning.
- [21] ACI 549 R-18. (2018). Report on ferrocement, American concrete institute (ACI), Detroit, Michigan, United States.
- [22] ACI 549.1R-18. (2018). Design guide for ferrocement, American concrete institute (ACI), Detroit, Michigan, United States.
- [23] Tanawade A. G. & Modhera C. D. (2017). Tensile Behaviour of Welded Wire Mesh and Hexagonal Metal Mesh for Ferrocement Application. *IOP Conf. Series: Materials Science and Engineering* 225. doi:10.1088/1757-899X/225/1/012069.
- [24] Somayaji S. & Shah S (1984). Prediction of tensile response of ferrocement. *Journal of Ferrocement*, 14(2).
- [25] Swamy, R.N. & Shaheen Y. (1990). Tensile behavior of thin reinforcement plates. *ACI, SP 124-18*, 356-387.